Confinement improvement with magnetic levitation of a superconducting dipole

D.T. Garnier[1]**, A.C. Boxer**[2]**, J.L. Ellsworth**[2]**, J. Kesner**[2] **and M.E. Mauel**[1]

[1] Department of Applied Physics, Columbia University, New York, NY 10027, USA
[2] Plasma Science and Fusion Center, Massachusetts Institute of Technology, Cambridge, MA 02139, USA

E-mail: dg276@columbia.edu

Abstract
We report the first production of high beta plasma confined in a fully levitated laboratory dipole using neutral gas fuelling and electron cyclotron resonance heating. As compared with previous studies in which the internal coil was supported, levitation results in improved confinement that allows higher-density, higher-beta discharges to be maintained at significantly reduced gas fuelling. Contrary to previous supported dipole plasma results which had the stored energy consisting in a hot electron population, a significant plasma stored energy is shown to reside in the bulk plasma. By eliminating supports used in previous studies, cross-field transport becomes the main loss channel for both the hot and the background species. This leads to a significant improvement in bulk plasma confinement and a dramatic peaking of the density profile. Improved particle confinement assures stability of the hot electron component at reduced neutral pressure.

(Some figures in this article are in colour only in the electronic version)

1. Introduction

The dipole confinement concept [1, 2] was motivated by spacecraft observations of planetary magnetospheres that show centrally peaked plasma pressure profiles forming naturally when the solar wind drives plasma circulation and heating. Unlike most other approaches to magnetic confinement in which stability requires average good curvature and magnetic shear, MHD stability in a dipole derives from plasma compressibility [3–5]. The marginal condition for stability is $\delta(pV^\gamma) = 0$, with p the plasma pressure, $V = \oint d\ell/B$ is the differential flux tube volume, and the adiabatic constant $\gamma = 5/3$. At marginal stability, an adiabatic exchange of flux tubes does not modify the pressure profile nor degrade energy confinement. Non-linear studies indicate that large-scale convective cells will form when the MHD stability limit is weakly violated, which results in the circulation of plasma between the hot core and the cooler edge region [6]. Studies have also predicted that the confined plasma can be stable to low-frequency (drift wave) modes when $\eta = d\ln T_e/d\ln n_e > 2/3$ [7]. The marginally stable case to both drift waves and MHD modes is thus where

$$p \propto V^{-\gamma} \quad \text{and} \quad n \propto V^{-1}. \tag{1}$$

This case corresponds to an equal number of particles and entropy per flux tube. These profiles are the expected result of sufficient interchange mixing [8], and they form the design basis for attractive dipole fusion reactor concepts [9].

The levitated dipole experiment (LDX), shown in figure 1, is investigating the confinement and stability of plasma in a dipole magnetic field configuration [10]. In the experiments reported here, high-beta plasma discharges were studied when the LDX high-field (3.5 T, 1.1 MAt) superconducting dipole magnet was levitated by attraction to a coil located above the vacuum chamber. (Local plasma β, where $\beta \equiv 2\mu_0 p/B^2$, has typically a peak value ∼25% in these fully poloidal magnetic field discharges [11].) This configuration utilizes a digital feedback system to obtain stable levitation of the floating coil. Experiments with the floating coil fully levitated began in 2007. Comparison 'supported mode' shots were taken with the cone shaped launching fixture raised to contact the inner section of the dipole and providing a loss mechanism for particles along all field lines.

In many experiments, the plasma was heated by 5 kW of electron cyclotron resonance heating (ECRH) evenly divided between 2.45 and 6.4 GHz. In other experiments, a third microwave source provided an additional 10 kW of heating at 10.5 GHz. This multi-frequency ECRH creates a two
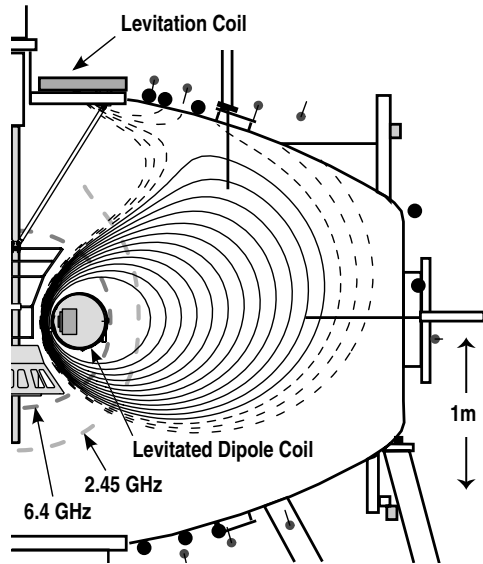
Figure 1. Schematic of the LDX device showing magnetic configuration and electron cyclotron resonance zones. Solid light lines are contours of magnetic flux in the closed field line region.

component plasma containing a hot electron species. For previously reported experiments with the dipole coil supported by thin supports, this results in a high-beta plasma with stored energy dominated by a population of energetic electrons with $E_{eh} > 50\,keV$ and $n_{eh} \sim 10^{16}\,m^{-3}$ [12].

2. Improved confinement with levitation

Figure 2 compares typical discharges in the supported and levitated modes of operation. A multi-chord interferometer is utilized to observe the background density profile [13]. For a similar level of fuelling resulting in similar vacuum pressure (figure 2(b)), we observe in the levitated mode a broader density profile and a higher overall density (figure 2(c)), indicative of improved confinement. In the afterglow, when the ECRH power is removed, a rapid plasma loss is seen in the supported mode as the plasma is lost to the supports. In the levitated operating mode a slow density decay is sometimes seen, matching the slow decay in the energetic particles.

The plasma diamagnetic flux (figure 2(d)), indicative of plasma stored energy, is doubled in the levitated mode of operation. This plasma stored energy, in supported operation contained in the hot electron population gives an idea of the improvement in confinement of the fast electrons which now must also be lost radially. Another indication of this cross-field hot electron transport was an observed heating of probes (located close to the plasma separatrix) up to temperatures at which they glow brightly ($\sim$2000 °C). This probe heating is not observed in supported experiments.

2.1. Energy confinement improvement

Figure 3 shows the relationship between chord averaged density and diamagnetic flux for levitated and supported plasmas. These plasmas were taken with a series of shots with 5 kW of heating (2.45 and 6.4 GHz sources). In both supported and levitated cases, there is an inverse relationship between
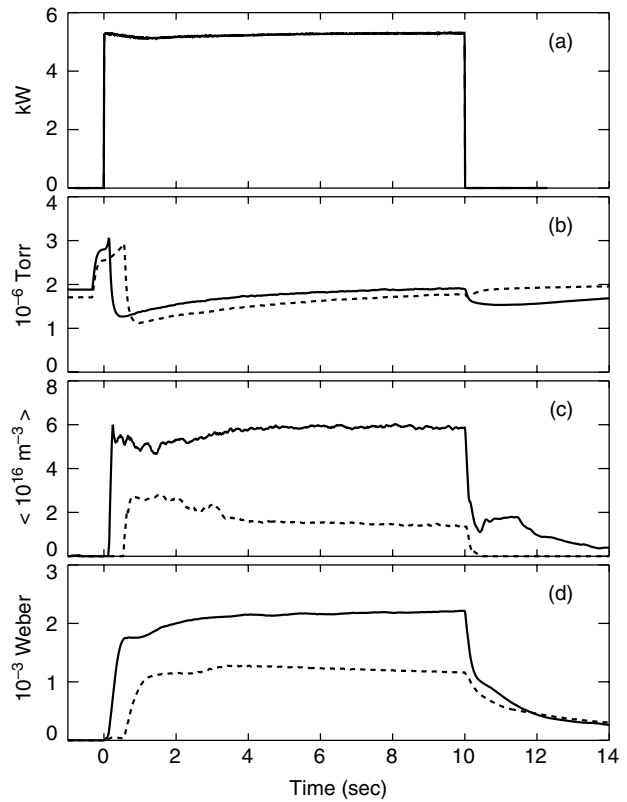

Figure 2. Wave forms for discharge in supported (dashed) and levitated (solid) mode: (*a*) RF power, (*b*) neutral pressure at external wall, (*c*) $R = 77$ cm density chord and (*d*) midplane diamagnetic signal.
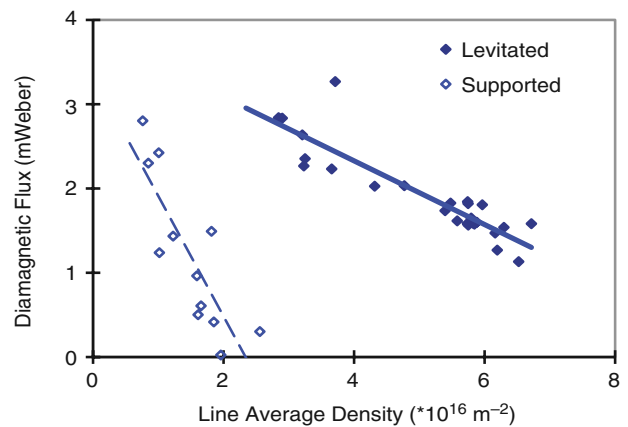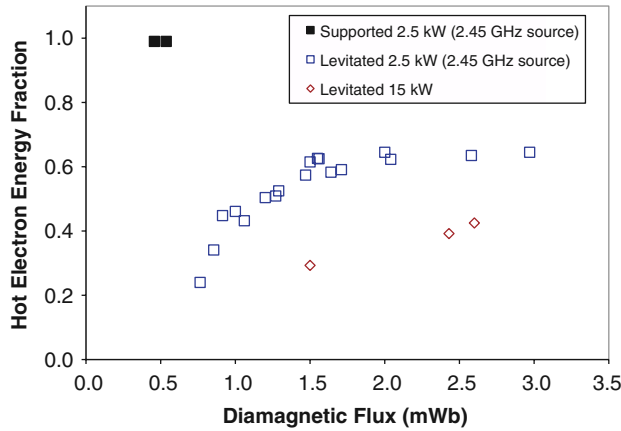

Figure 3. Diamagnetic flux for supported and levitated operation during density scan of run 80321. Total input power is 5 kW. Both operations show an inverse scaling between global energy confinement and bulk density.

density and stored energy. This inverse relationship, consistent with collisional transport, indicates a marked improvement with levitation.

As previously reported [12], the stored energy in supported plasmas resides in the energetic electron population. Returning to figure 2(*d*), we see for the supported case the normal (slow) exponential fall off of stored energy associated with the decay of the low collisionality fast electrons during the afterglow. However, for the levitated case, there appears to be
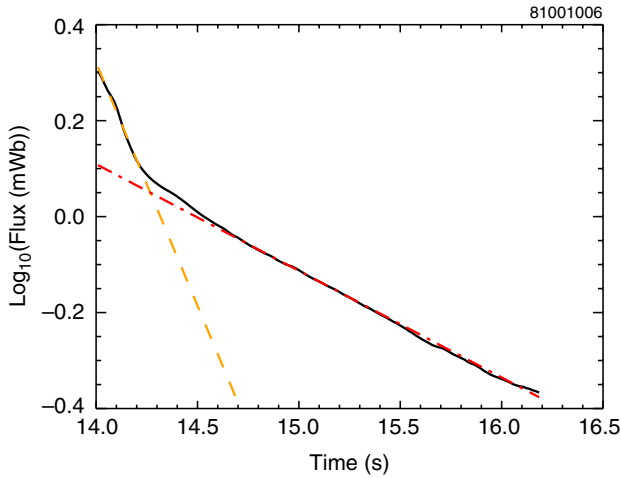
Figure 4. Logarithm of diamagnetic flux decay during the afterglow of a levitated plasma shot. As is typical of levitated shots, the energy shows two distinct decay rates, indicating a warm bulk plasma and an energetic hot electron population. Exponential fits to the decays are shown in dashed lines.

Figure 5. Fraction of stored energy consisting of hot electrons for supported and levitated plasmas, as computed from decay of diamagnetic flux during afterglow. The closed symbols are supported shots, while open ones are for levitated cases.

two distinct decay rates, which much of the additional stored energy consisting in the new faster decaying population.

Figure 4 shows a logarithmic plot of the afterglow stored energy decay of a levitated plasma. The decay can be fitted to two distinct exponential decays with remarkable clarity. For this case, LDX Shot 8101006, the faster decay, which we associate with the warm bulk plasma is $\tau_{\mathrm{warm}} \sim 400$ ms. The slower decay is similar to that seen with supported plasmas at the same neutral pressure and is $\tau_{\mathrm{hot}} \sim 2$ s.

Using the two fits to the diamagnetic decay, and extending the fits back to the beginning of the afterglow period, we can estimate the proportion of energy in each population during the main heating period. Shown in figure 5 is the ratio of the stored energy consisting in the hot electron plasma to the total stored energy for a variety of conditions. Here we see again that supported plasmas have energy only in the hot electron component. However, for levitated plasmas, the hot component makes up at most 60% of the total stored energy, and is less than 1/2 of the stored energy for 15 kW heated

plasmas. Thus we see that with levitation, a significant amount of the plasma beta is stored in the bulk plasma. As an aside, we note this bulk plasma has an energy confinement time in the afterglow period from between 100 and 500 ms. This should be compared with the measured confinement time during heating of between 50–100 ms as measured by reconstruction of the equilibrium stored energy divided by the input power.

While the hot electron confinement is improved for similar conditions, it is much less than the dramatic improvement in the bulk plasma confinement. During the supported operations, hot electrons are mirror trapped and are lost on a pitch angle scattering time to the supports. By levitating, the fast particles should become more isotropic when scattered, and not be lost. However, the slowing down time for the hot electrons is nearly the same as the pitch angle scattering time; 5.2 s and 4.3 s respectively for $n_{\mathrm{e}} = 10^{17}\,\mathrm{m}^{-3}$ and $T_{\mathrm{hot}} = 200$ keV. Combined with higher bulk density, this may limit the fraction of energy residing in the hot electron population while levitated. We also note that field errors may enhance fast passing particle radial transport [14].

2.2. Particle confinement improvement

Data from a collection of shots with different conditions give a statistical picture of the same improvement in particle confinement. Shown in figure 6 is line density as a function of neutral pressure from the inner most chord of the interferometer with a a tangency radius of 0.77 m. While the line average density increases with neutral gas fuelling and with increasing microwave power, the data show a 2–3 fold increase as the mechanical supports are withdrawn from the plasma.

Figure 6 also shows a positive mass scaling to confinement at higher fuelling rates, which we believe indicates the rate-limiting role of edge plasma loss on open field lines beyond the magnetic separatrix. Specifically, if we assume marginal profiles where input power is lost by the power flow along field lines in the scrape-off-layer, we obtain [15]

$$\frac{(1 - f_{\mathrm{R}}) p_0 V_0}{\tau_{\mathrm{E}}} \approx 2 p_{\mathrm{sol}} A_{\mathrm{sol}} c_{\mathrm{s}}, \tag{2}$$

where f_{R} is the fraction of radiated power, subscripts 0 and sol indicate peak and scrape-off-layer values, A_{sol} is the scrape-off-layer area and c_{s} is the sound speed. Thus, higher confinement of the slower He plasma is consistent with this simple model. The figure also shows an interesting optimum in density for D_2 fuelling. We speculate that this is due to increased radiated power (specifically charge exchange losses) with higher neutral particle density.

2.3. Observation of peaked density profiles

A four channel interferometer [13] was used to monitor the time evolution of the density profile and the change in density profile resulting from magnetic levitation of the superconducting dipole. One approximate and appropriate method to reconstruct the density profile from the line density measured by the interferometer array is to use a piece-wise model for the plasma density profile, which takes the density to vary as $n \propto V^{-1}$ between the interferometer chords. A least squares *t* of this form of the profile with the interferometer
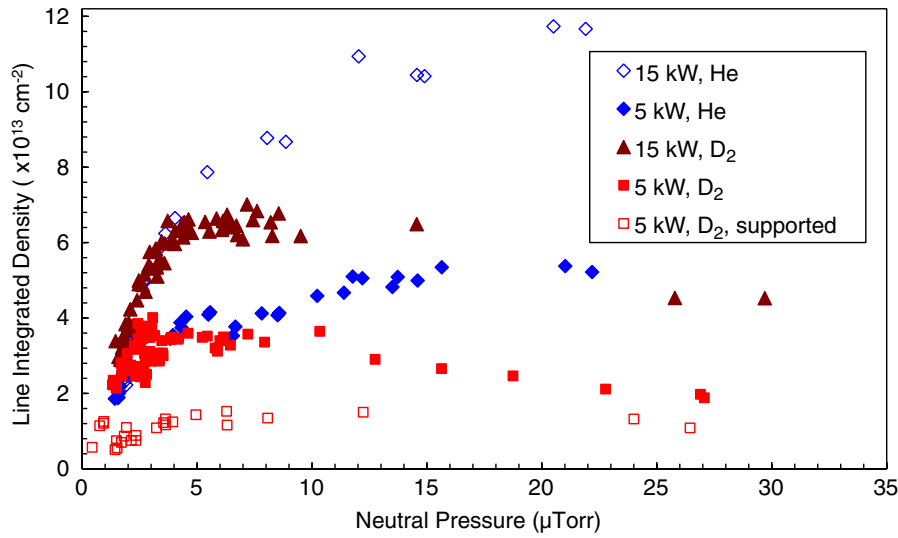
Figure 6. Steady state chordal density measurement versus neutral pressure for different conditions. The effect of levitation for deuterium plasmas with 5 kW of input ECRH is shown as increased density by a factor of 2–4. (Also depicted are significant power and species dependencies at high neutral pressure.)
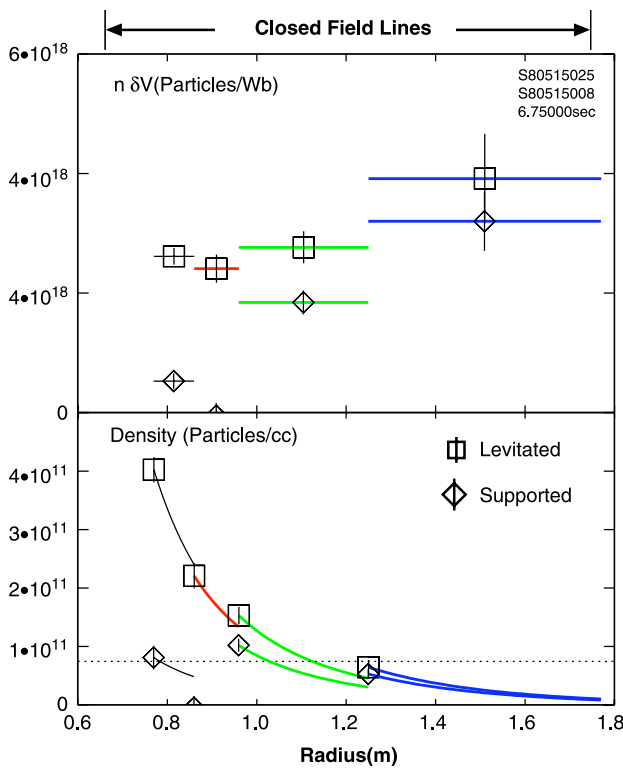
Figure 7. Computation of the density profile for supported (diamond) and levitated (square) discharges under similiar conditions with 15 kW of ECRH.

measurements determines a best fit density profile. By making different assumptions about the shape of the density profile, different reconstructions can also fit measurements; however, the general shape of the reconstructed profiles remain the same in each case.

Figure 7 compares the density profile from two similar discharges at 15 kW ECRH power. When the dipole coil is levitated, the central density is highly peaked and at least four-times larger than the central density obtained with a supported dipole. With supports, the density profile is hollow, indicative of the parallel loss of plasma between radially localized source regions. We note that for the levitated case the assumption of $nV = $ constant, appears justified over much of the plasma. This expected observation has significant consequences for the dipole concept.

3. Low-frequency fluctuations in levitated plasmas

Plasma confinement with a levitated dipole is dominated by radial transport, and levitated experiments have permitted the exploration of the dynamics and transport of plasma confined in a magnetic configuration relevant to a potential dipole fusion reactor. The partially ionized edge background plasma in LDX has $n_e \sim 0.2$–$5 \times 10^{16}\, m^{-3}$, $T_e \sim 10$–$20\, eV$. With magnetic field as low as $B \gtrsim 0.1\, mT$, the magnetic Lundquist number, $S \equiv \mu_0 L V_A / \eta$, where L is a characteristic scale length, V_A is the Alfven speed and η is the plasma resistivity, is between 10^4 and 10^6. We observe fluctuations in the diamagnetic drift frequency range (0.2–10 kHz) that are effected by the rate of neutral fuelling. Similarly to previous observations [16], large-scale and low toroidal wave number are observed. In levitated plasmas, the modes exhibit a radial structure with different frequencies seen across the discharge.

These low-frequency fluctuations co-exist with the high-beta fast electrons but are most probably associated with convective and/or drift-wave-like modes of the cooler background plasma. For typical discharges, low-frequency fluctuations are always observed and may indicate the nature of the plasma electrostatic interchange-like convection that is responsible for peaked profiles with $n \propto V^{-1}$.

4. Improved stability to hot electron interchange (HEI)

The hot electron species can be unstable to the HEI [17–19] mode when the hot electron density gradient is sufficiently high

and the background density is sufficiently low [12]. In prior supported mode experiments if neutral particle fuelling was too low, the plasma would be in a low density, low beta, unstable state. If sufficient neutral particle fuelling was supplied, the plasma would become stable and then density and beta would rise dramatically. However, if sufficient fuelling was not maintained, the plasma could become radically unstable leading to a loss of all plasma stored energy.

Similarly to supported mode operation, when the dipole is levitated the plasma entered a high-density regime in which the HEI was stabilized for sufficient gas fuelling. However, the plasma is now maintained in the high-density regime when the gas fuelling is substantially reduced as compared with the supported mode. In fact, we have not yet observed a case in levitated operation when high-beta discharges are subject to fast, large-scale instabilities during the heated plasma operations. Additionally, in supported plasmas limiting HEI activity is often observed, where HEI occur but lead to small scale bursts of outward energy transport and limit the total stored energy. This behaviour is seldom observed during levitated dipole operation. Only in recent experiments with 15 kW of input power, and neutral pressure below 1 μTorr, have we observed these small intermittent bursts of HEI. We believe the enhanced stability of the HEI during levitation results from both a radial transport broadened hot electron profile and a higher core plasma density resulting from improved particle confinement.

5. Summary

We report the first production of high-beta plasma confined by a levitated superconducting dipole magnet. As compared with previous studies in which the internal coil was supported [12], levitation results in improved particle confinement that allows high-density, high-beta discharges to be maintained at significantly reduced gas fuelling. Elimination of parallel losses coupled with reduced gas leads, to improved energy confinement and a dramatic change in the density profile. In levitated plasmas, a warm plasma component contains a significant portion of the plasma stored energy. Improved particle confinement assures stability of the hot electron component at reduced pressure. By eliminating the supports used in previous studies, cross-field transport becomes the main loss channel for both the hot and the background species.

Acknowledgments

References

[1] Hasegawa A. 1987 A dipole field fusion reactor *Comments Plasma Phys. Control. Fusion* **11** 147–51

[2] Hasegawa A., Chen L. and Mauel M.E. 1990 A D-He-3 fusion-reactor based on a dipole magnetic-field *Nucl. Fusion* **30** 2405–13

[3] Rosenbluth M.N. and Longmuire C.L. 1957 Stability of plasmas confined by magnetic fields *Ann. Phys.* **1** 120–40

[4] Gold T. 1959 Motions in the magnetosphere of the earth *J. Geophys. Res.* **47** 1219–24

[5] Garnier D.T., Kesner J. and Mauel M.E. 1999 Magnetohydrodynamic stability in a levitated dipole *Phys. Plasmas* **6** 3431–4

[6] Pastukhov V.P. and Chudin N.V. 2001 Plasma convection near the threshold for MHD instability in nonparaxial magnetic confinement systems *Plasma Phys. Rep.* **27** 907–21

[7] Kesner J. and Hastie R.J. 2002 Electrostatic drift modes in a closed field line configuration *Phys. Plasmas* **9** 395–400

[8] Kouznetsov A., Freidberg J.P. and Kesner J. 2007 Quasilinear theory of interchange modes in a closed field line configuration *Phys. Plasmas* **14** 102501

[9] Kesner J., Garnier D.T., Hansen A., Mauel M. and Bromberg L. 2004 Helium catalysed D–D fusion in a levitated dipole *Nucl. Fusion* **44** 193–203

[10] Garnier D.T. *et al* 2006 Design and initial operation of the LDX facility *Fusion Eng. Des.* **81** 2371–80

[11] Karim I., Mauel M.E., Ellsworth J.L., Boxer A.C., Garnier D.T., Hansen A.K., Kesner J. and Ortiz E.E. 2007 Equilibrium reconstruction of anisotropic pressure profile in the Levitated Dipole Experiment *J. Fusion Energy* **26** 99–102

[12] Garnier D.T., Hansen A.K., Mauel M.E., Ortiz E.E., Boxer A.C., Ellsworth J.L., Karim I., Kesner J., Mahar S. and Roach A. 2006 Production and study of high-beta plasma confined by a superconducting dipole magnet *Phys. Plasmas* **13** 056111

[13] Boxer A.C., Garnier D.T. and Mauel M.E. 2009 Multichannel microwave interferometer for the levitated dipole experiment *Rev. Sci. Instrum.* **80** 043502

[14] Ryutov D.D., Kesner J. and Mauel M.E. 2004 Magnetic field perturbations in closed-field-line systems with zero toroidal magnetic field *Phys. Plasmas* **11** 2318–21

[15] Kesner J. and Mauel M.E. 1997 Plasma confinement in a levitated magnetic dipole *Plasma Phys. Rep.* **23** 742–50

[16] Garnier D.T., Boxer A.C., Ellsworth J.L., Hansen A.K., Karim I., Kesner J., Mauel M.E., Ortiz E.E. and Roach A. 2008 Stabilization of a low-frequency instability in a dipole plasma *J. Plasma Phys.* **74** 733–40

[17] Krall N.A. 1966 Stabilization of hot electron plasma by a cold background *Phys. Fluids* **9** 820–1

[18] Levitt B., Maslovsky D.A. and Mauel M.E. 2002 Measurement of the global structure of interchange modes driven by energetic electrons trapped in a magnetic dipole *Phys. Plasmas* **9** 2507–17

[19] Krasheninnikova N.S. and Catto P.J. 2005 Effects of hot electrons on the stability of a closed field line plasma *Phys. Plasmas* **12** 032101